INTERNATIONAL JOURNAL FOR NUMERICAL METHODS IN ENGINEERING, VOL. 37, 645–667 (1994)

ON STABILITY AND CONVERGENCE OF FINITE ELEMENT APPROXIMATIONS OF BIOT'S CONSOLIDATION PROBLEM

MÁRCIO A. MURAD AND ABIMAEL F. D. LOULA

Laboratório Nacional de Computação Científica - LNCC/CNPq Rua Lauro Muller 455, 22290—Rio de Janeiro, Brazil

SUMMARY

Stability and convergence analysis of finite element approximations of Biot's equations governing quasi-static consolidation of saturated porous media are discussed. A family of decay functions, parametrized by the number of time steps, is derived for the fully discrete backward Euler–Galerkin formulation, showing that the pore-pressure oscillations, arising from an unstable approximation of the incompressibility constraint on the initial condition, decay in time. Error estimates holding over the unbounded time domain for both semidiscrete and fully discrete formulations are presented, and a post-processing technique is employed to improve the pore-pressure accuracy.

1. INTRODUCTION

Variational principles and finite element approximations for Biot's quasi-static consolidation theory [1–4] have been proposed by many investigators [5–11] from the view point of applications to Geomechanics. To solve this problem, time-stepping integration schemes, whose stability and accuracy are discussed in References 12–14, are usually employed, combined with finite element approximation in the space domain. Galerkin finite element approximations of Biot's equations in terms of soil displacement and pore pressure have presented spurious oscillations in the pressure field in the early stage of the consolidation process[15–17] for some combinations of displacement and pore-pressure finite element spaces, specially those with equal order of interpolation. To avoid this misbehaviour, different orders of interpolation, usually one order lower for pore pressure compared to displacements or reduced integration techniques,[16] have been adopted. This lack of stability close to the initial-time results from an unstable approximation of the initial condition. At $t = 0$, we shall solve an incompressible elasticity problem (same structure of Stokes flow) in displacement and pore-pressure formulation whose finite element approximation must satisfy the Babuška–Brezzi condition (see, e.g. References 18–21).

The analysis of the influence of error in the initial data over stable and unstable approximations of Biot's problem is the main goal of the present article. In a previous paper,[22] by applying established techniques of numerical analysis of parabolic problems,[23] we derived error estimates for both semidiscrete and fully discrete backward Euler–Galerkin approximations of Biot's consolidation problem. However, these estimates contain error constants that increase with time, so their validity remains limited to a finite time interval $(0, T]$. For the semidiscrete Galerkin formulation, we obtained an exponential decay of the error in the initial data in time and proposed sequential Galerkin/Petrov Galerkin post-processing techniques to improve the

0029-5981/94/040645-23$16.50

Received 17 February 1992
Revised 24 April 1993

accuracy of pore pressure and effective stresses approximations. Here, we generalize the decay result obtained in Reference 22 to the fully discrete backward Euler–Galerkin approximation of Biot's consolidation problem and derive sharper error estimates holding over the unbounded time domain for both semidiscrete and fully discrete formulations. A family of decay functions parametrized by the number of time steps m, whose limit as $m \to \infty$ recovers the semidiscrete case is presented. To improve the pore-pressure approximation, a post-processing is adopted, based on the momentum equation for the fluid, with the same order of displacements.

To illustrate the analysis, numerical simulations of the classical one-dimensional column and two-dimensional strip-load problems are performed. Comparisons of accuracy and convergence rates between stable, unstable and post-processed pore pressures are presented for the classical one-dimensional example. In the bidimensional consolidation example, the time histories of pore-pressure oscillations are presented, and the influence of the time step on the decay function and the performance of the post processing approach is discussed.

A brief outline of the paper is as follows. In Section 2 we review strong and weak formulations of Biot's consolidation problem in terms of displacements of the porous medium and pore-pressure fields. The nature of the initial, evolutionary and stationary problems are emphasized. In Section 3 we present the semidiscrete Galerkin approximation and review the results of Reference 22 related to the exponential decay of initial data error in time. In Section 4, exploring the consequences of the decay result, we derive sharp error estimates, valid for the unbounded time domain, for both stable and unstable methods. In Section 5 we generalize the previous methodology of analysis, deriving a family of decay functions for the fully discrete backward Euler–Galerkin approximation. In Section 6 we present the post-processing approach and illustrative results of numerical experiments are shown in Section 7.

2. PRELIMINARIES

For simplicity, we consider $\Omega \subset \mathbb{R}^2$ with smooth boundary Γ and unit outward normal $\mathbf{n}$. Neglecting body forces, the classical Biot's problem governing quasi-static consolidation of saturated porous media consists in finding, for each time $t \in (0, \infty)$, the displacement of the porous medium $\mathbf{u}: \Omega \to \mathbb{R}^2$ and the pore pressure $p: \Omega \to \mathbb{R}$ such that

$$\mu \nabla^2 \mathbf{u} + (\lambda + \mu) \nabla \operatorname{div} \mathbf{u} - \nabla p = 0 \quad \text{in } \Omega \tag{1}$$

$$\operatorname{div} \mathbf{u}_t - \frac{\kappa}{\eta} \nabla^2 p = 0 \quad \text{in } \Omega \tag{2}$$

with the initial condition given by

$$\operatorname{div} \mathbf{u} = 0 \text{ in } \Omega, \quad t = 0 \tag{3}$$

and the boundary conditions of the type

$$\mathbf{u} = 0, \quad \frac{\kappa}{\eta} \nabla p \cdot \mathbf{n} = Q \quad \text{on } \Gamma_1 \tag{4}$$

$$p = 0, \quad (\lambda \operatorname{div} \mathbf{u} \mathbf{I} + 2\mu \boldsymbol{\varepsilon}(\mathbf{u}))\mathbf{n} = \mathbf{h} \quad \text{on } \Gamma_2 \tag{5}$$

where $\Gamma_1 \cup \Gamma_2 = \Gamma$, with Γ_1 and Γ_2 disjoint subsets of Γ, λ and μ are the Lamé constants, κ is the permeability of the porous skeleton, η is the viscosity of the pore fluid, $\boldsymbol{\varepsilon}(\mathbf{u}) = 1/2(\nabla \mathbf{u} + \nabla \mathbf{u}^{\mathrm{T}})$ and the subscript t denotes time derivative. For simplicity, we consider only non-homogeneous boundary conditions of the Newman type, measured by the functions $\mathbf{h}$ and Q, denoting, respectively, the prescribed traction and discharge on the boundary.

The stability analysis of finite element approximations of the proposed problem is motivated by the nature of the initial condition (3), which expresses the incompressible response of the solid–fluid aggregate in the beginning of the consolidation process.

To present the variational formulation of the proposed problem, we first define the appropriate function spaces. Let $L^2(\Omega)$ be the set of square-integrable scalar-valued functions defined on Ω, with inner product

$$(f, g) = \int_\Omega fg \, \mathrm{d}\Omega \quad \forall f, g \in L^2(\Omega) \tag{6}$$

equipped with the norm

$$\| f \| = (f, f)^{1/2} \tag{7}$$

Let $\partial^\alpha f$ denote the following derivative of f, in the sense of distributions.

$$\partial^\alpha f = \frac{\partial^{|\alpha|} f}{\partial x_1^{\alpha_1} \, \partial x_2^{\alpha_2}} \tag{8}$$

with α_i a natural integer and $|\alpha| = \alpha_1 + \alpha_2$. Let $H^m(\Omega)$ denote the Hilbert space

$$H^m(\Omega) = \{ f \in L^2(\Omega); \ \forall \alpha, |\alpha| \leqslant m, \partial^\alpha f \in L^2(\Omega) \} \tag{9}$$

with inner product

$$(f, g)_m = \sum_{|\alpha| \leqslant m} \int_\Omega \partial^\alpha f \partial^\alpha g \, \mathrm{d}\Omega \quad \forall f, g \in H^m(\Omega) \tag{10}$$

norm

$$\| f \|_m = (f, f)_m^{1/2} \tag{11}$$

and seminorm

$$|f|_m = \left(\sum_{|\alpha| = m} (\partial^\alpha f, \partial^\alpha f) \right)^{1/2} \tag{12}$$

Let

$$U = \{ \mathbf{f} \in H^1(\Omega) \times H^1(\Omega), \mathbf{f} = \mathbf{0} \text{ on } \Gamma_1 \} \tag{13}$$

be the space of displacement field, and

$$V = \{ g \in H^1(\Omega), g = 0 \text{ on } \Gamma_2 \} \tag{14}$$

be the pore-pressure space. The nature of the variational problem associated with Biot's equations changes according to the different stages of the consolidation process. The initial configuration of the saturated mixture is usually obtained by combining the equilibrium equation (1) with the constraint (3), which means that the mixture responds initially like an incompressible medium governed by Stokes' equations whose variational form is given as follows.

Problem M_0. Find $\{\mathbf{u}(0), p(0)\} \in U \times L^2(\Omega)$ such that

$$2\mu(\boldsymbol{\varepsilon}(\mathbf{u}(0)), \boldsymbol{\varepsilon}(\mathbf{v})) - (p(0), \operatorname{div} \mathbf{v}) = f(\mathbf{v}) \quad \forall \mathbf{v} \in U \tag{15}$$

$$(\operatorname{div} \mathbf{u}(0), q) = 0 \quad \forall q \in L^2(\Omega) \tag{16}$$

with

$$f(\mathbf{v}) = \int_{\Gamma_2} \mathbf{h} \cdot \mathbf{v} \, \mathrm{d}\Gamma \tag{17}$$

while the variational formulation of the evolutionary consolidation problem consists in

Problem M_t. For each $t \in (0, \infty)$, find $\{\mathbf{u}(t), p(t)\} \in U \times V$ such that

$$2\mu(\boldsymbol{\varepsilon}(\mathbf{u}), \boldsymbol{\varepsilon}(\mathbf{v})) + \lambda(\operatorname{div} \mathbf{u}, \operatorname{div} \mathbf{v}) - (p, \operatorname{div} \mathbf{v}) = f(\mathbf{v}) \quad \forall \mathbf{v} \in U \tag{18}$$

$$(\operatorname{div} \mathbf{u}_t, q) + \frac{\kappa}{\eta}(\nabla p, \nabla q) = g(q) \quad \forall q \in V \tag{19}$$

with $f(\mathbf{v})$ given by (17), $\{\mathbf{u}(0), p(0)\}$ solution of M_0, and

$$g(q) = \int_{\Gamma_1} Qq \, \mathrm{d}\Gamma \tag{20}$$

For the stationary consolidation problem, obtained by dropping the term $(\operatorname{div} \mathbf{u}_t, q)$ in (19), we have the following decoupled formulation.

Problem M_∞. Find $\{\mathbf{u}, p\} \in U \times V$ such that

$$2\mu(\boldsymbol{\varepsilon}(\mathbf{u}), \boldsymbol{\varepsilon}(\mathbf{v})) + \lambda(\operatorname{div} \mathbf{u}, \operatorname{div} \mathbf{v}) - (p, \operatorname{div} \mathbf{v}) = f(\mathbf{v}) \quad \forall \mathbf{v} \in U \tag{21}$$

$$\frac{\kappa}{\eta}(\nabla p, \nabla q) = g(q) \quad \forall q \in V \tag{22}$$

The previous sequence of variational problems defines different stages in the consolidation process. From (15)–(22), we note that the nature of the pore-pressure field changes from a Lagrange multiplier in a saddle-point problem (M_0) to a potential satisfying Poisson equation (M_∞). This fact leads to the conclusion that stabilization in the pore-pressure field occurs as a consequence of the consolidation process (M_t).

3. SEMIDISCRETE GALERKIN ANALYSIS

For simplicity, we admit that Ω is a polygonal domain uniformly discretized by a finite element mesh of Ne elements, with mesh parameter h. Let $S_h^k \subset H^1(\Omega)$ be the spaces of C^0 piecewise polynomial finite element interpolations of degrees k (triangles or quadrilaterals). Considering $U_h^k = \{S_h^k \times S_h^k\} \cap U$ and $V_h^l = S_h^l \cap V$, the semidiscrete Galerkin approximation for problem M_t reads

Problem M_{ht}. For each $t \in (0, \infty)$, find $\{\mathbf{u}_h(t), p_h(t)\} \in U_h^k \times V_h^l$ such that

$$2\mu(\boldsymbol{\varepsilon}(\mathbf{u}_h), \boldsymbol{\varepsilon}(\mathbf{v}_h)) + \lambda(\operatorname{div} \mathbf{u}_h, \operatorname{div} \mathbf{v}_h) - (p_h, \operatorname{div} \mathbf{v}_h) = f(\mathbf{v}_h) \quad \forall \mathbf{v}_h \in U_h^k \tag{23}$$

$$(\operatorname{div} \mathbf{u}_{ht}, q_h) + \frac{\kappa}{\eta}(\nabla p_h, \nabla q_h) = g(q_h) \quad \forall q_h \in V_h^l \tag{24}$$

with $\mathbf{u}_h(0)$ and $p_h(0)$ satisfying

M_{h0}.

$$2\mu(\boldsymbol{\varepsilon}(\mathbf{u}_h(0)), \boldsymbol{\varepsilon}(\mathbf{v}_h)) - (p_h(0), \operatorname{div} \mathbf{v}_h) = f(\mathbf{v}_h) \quad \forall \mathbf{v}_h \in U_h^k \tag{25}$$

$$(\operatorname{div} \mathbf{u}_h(0), q_h) = 0 \quad \forall q_h \in V_h^l \tag{26}$$

From Brezzi's theorem,[18] the stability of M_{h0} depends on the inf–sup or LBB condition

LBB. There exists $\beta > 0$, independent of h, such that

$$\sup_{\mathbf{v}_h \in U_h^k} \frac{(\operatorname{div} \mathbf{v}_h, q_h)}{\|\nabla \mathbf{v}_h\|} \geqslant \beta \|q_h\| \quad \forall q_h \in V_h^l \tag{27}$$

For continuous pore-pressure interpolation, the choice $k = l + 1$, corresponding to Taylor–Hood elements,[24] verifies (27) and leads to stable and optimally convergent solution of $\mathbf{M}_{h0}$. Unstable approximations of $\mathbf{M}_{h0}$, not satisfying (27) ($k = l$, for example), may destroy the uniqueness of the pore-pressure approximation $p_h(0)$. The main question we intend to discuss here is: *What is the influence of the error in the initial data (M_{h0}) upon the approximate solution of the quasi-static consolidation problem (M_{ht})?* To answer this question we shall enter into the field of numerical analysis of parabolic problems. Applying the methodology presented in Reference 23 for the heat equation, in Reference 22 we presented an analysis of problem $\mathbf{M}_{ht}$, based on the definition of a comparison function, namely the elliptic projection $\{\bar{\mathbf{u}}_h(t), \bar{p}_h(t)\} \in U_h^k \times V_h^l$ of $\{\mathbf{u}(t), p(t)\}$, given by the solution of the following decoupled elliptic problems:

$$2\mu(\boldsymbol{\varepsilon}(\bar{\mathbf{u}}_h), \boldsymbol{\varepsilon}(\mathbf{v}_h)) + \lambda(\operatorname{div} \bar{\mathbf{u}}_h, \operatorname{div} \mathbf{v}_h) - (\bar{p}_h, \operatorname{div} \mathbf{v}_h) = 2\mu(\boldsymbol{\varepsilon}(\mathbf{u}), \boldsymbol{\varepsilon}(\mathbf{v}_h)) + \lambda(\operatorname{div} \mathbf{u}, \operatorname{div} \mathbf{v}_h) - (p, \operatorname{div} \mathbf{v}_h) \quad \forall \mathbf{v}_h \in U_h^k \tag{28}$$

$$(\nabla \bar{p}_h, \nabla q_h) = (\nabla p, \nabla q_h) \quad \forall q_h \in V_h^l \tag{29}$$

The errors $\mathbf{u} - \mathbf{u}_h$ and $p - p_h$ are separated in two parts. The first, $\boldsymbol{\rho}_u$ and ρ_p, results from the difference between the exact solution and the elliptic projection. The second, $\mathbf{e}_u$ and the e_p, is the difference between the approximate solution and the elliptic projection. By the triangle inequality we have

$$\|\mathbf{u} - \mathbf{u}_h\| = \|\mathbf{u} - \bar{\mathbf{u}}_h + \bar{\mathbf{u}}_h - \mathbf{u}_h\| \leqslant \|\boldsymbol{\rho}_u\| + \|\mathbf{e}_u\| \tag{30}$$

$$\|p - p_h\| = \|p - \bar{p}_h + \bar{p}_h - p_h\| \leqslant \|\rho_p\| + \|e_p\| \tag{31}$$

From (29), ρ_p can easily be estimated using the well-known results for Poisson's equation (see, e.g. Reference 25) as follows:

$$\|\rho_p\| \leqslant Ch^{l+1}|p|_{l+1}; \qquad \|\nabla \rho_p\| \leqslant Ch^l|p|_{l+1} \tag{32}$$

Thus (32) can be used in (28) to estimate $\|\boldsymbol{\rho}_u\|$. Applying the procedure presented in Reference 22 we get

$$\|\boldsymbol{\rho}_u\| \leqslant Ch^{s+1}(|\mathbf{u}|_{k+1} + |p|_{l+1}); \quad \|\boldsymbol{\varepsilon}(\boldsymbol{\rho}_u)\| \leqslant Ch^s(|\mathbf{u}|_{k+1} + |p|_{l+1}) \tag{33}$$

with $s = \min(k, l + 1)$. Using the fact that

$$\|\operatorname{div} \mathbf{v}\| = \sqrt{2}\,\|\boldsymbol{\varepsilon}(\mathbf{v})\| \tag{34}$$

and Korn's inequality,

$$\|\boldsymbol{\varepsilon}(\mathbf{v})\| \geqslant C\|\nabla \mathbf{v}\| \tag{35}$$

with $C > 0$, the estimate for $\|\boldsymbol{\varepsilon}(\boldsymbol{\rho}_u)\|$ also holds for $\|\nabla \boldsymbol{\rho}_u\|$ and $\|\operatorname{div} \boldsymbol{\rho}_u\|$.

Estimates (32) and (33) are independent of any compatibility condition (like (27)) between U_h^k and V_h^l. Therefore, the Galerkin approximation of problem $\mathbf{M}_\infty$ converges for any combination of conforming finite element spaces.

For the time derivatives of the elliptic projection we also have

$$\|\operatorname{div} \boldsymbol{\rho}_{u_t}\| \leqslant Ch^s(|\mathbf{u}_t|_{n+1} + |p_t|_{n+1}) \tag{36}$$

$$\|\operatorname{div} \boldsymbol{\rho}_{u_{tt}}\| \leqslant Ch^s(|\mathbf{u}_{tt}|_{n+1} + |p_{tt}|_{n+1}) \tag{37}$$

It remains to estimate $\mathbf{e}_u$ and e_p. Considering the definition of the elliptic projection (28), (29) and problems $\mathbf{M}_t$ and $\mathbf{M}_{ht}$, a variational error equation coupling them with $\boldsymbol{\rho}_u$ can be obtained in the following form:

$$2\mu(\boldsymbol{\varepsilon}(\mathbf{e}_{\mathbf{u}}), \boldsymbol{\varepsilon}(\mathbf{v}_h)) + \lambda(\operatorname{div} \mathbf{e}_{\mathbf{u}}, \operatorname{div} \mathbf{v}_h) - (e_p, \operatorname{div} \mathbf{v}_h) = 0 \quad \forall \mathbf{v}_h \in U_h^k \tag{38}$$

$$(\operatorname{div} \mathbf{e}_{\mathbf{u}_t}, q_h) + \frac{\kappa}{\eta}(\nabla e_p, \nabla q_h) = (\operatorname{div} \boldsymbol{\rho}_{\mathbf{u}_t}, q_h) \quad \forall q_h \in V_h^l \tag{39}$$

For appropriate choices of $\mathbf{v}_h$ and q_h, the left-hand side of (38) and (39) can be bounded by the right-hand side, previously estimated in (36). Adopting this procedure we can derive the following decay result (see Reference 22):

$$\frac{\mathrm{d}}{\mathrm{d}t} E(t) + C_1 E(t) \leqslant C_2(\|\operatorname{div} \boldsymbol{\rho}_{\mathbf{u}_t}\|^2 + \|\operatorname{div} \boldsymbol{\rho}_{\mathbf{u}_{tt}}\|^2) \tag{40}$$

in which

$$E = \|\boldsymbol{\varepsilon}(\mathbf{e}_{\mathbf{u}})\|^2 + \|\operatorname{div} \mathbf{e}_{\mathbf{u}}\|^2 + \|\nabla e_p\|^2 + \|\boldsymbol{\varepsilon}(\mathbf{e}_{\mathbf{u}_t})\|^2 + \|\operatorname{div}(\mathbf{e}_{\mathbf{u}_t})\|^2 \tag{41}$$

and C_1, C_2 are positive constants. Inequality (40) admits an integration factor $\exp(C_1 t)$ implying in the following decay of the initial data error in time:

$$E(t) \leqslant E(0)\exp(-C_1 t) + \int_0^t (\|\operatorname{div} \boldsymbol{\rho}_{\mathbf{u}_t}\|^2 + \|\operatorname{div} \boldsymbol{\rho}_{\mathbf{u}_{tt}}\|^2)\exp(C_1(t-\tau))\,\mathrm{d}\tau \tag{42}$$

Noting that

$$\begin{aligned}
&\int_0^t (\|\operatorname{div} \boldsymbol{\rho}_{\mathbf{u}_t}\|^2 + \|\operatorname{div} \boldsymbol{\rho}_{\mathbf{u}_{tt}}\|^2)\exp(-C_1(t-\tau))\,\mathrm{d}\tau \\
&\leqslant \sup_{\tau \leqslant t}(\|\operatorname{div} \boldsymbol{\rho}_{\mathbf{u}_t}(\tau)\|^2 + \|\operatorname{div} \boldsymbol{\rho}_{\mathbf{u}_{tt}}(\tau)\|^2)\int_0^t \exp(-C_1(t-\tau))\,\mathrm{d}\tau \\
&= \sup_{\tau \leqslant t}(\|\operatorname{div} \boldsymbol{\rho}_{\mathbf{u}_t}(\tau)\|^2 + \|\operatorname{div} \boldsymbol{\rho}_{\mathbf{u}_{tt}}(\tau)\|^2)\left(\frac{1-\exp(-C_1 t)}{C_1}\right) \\
&\leqslant \frac{1}{C_1}\sup_{\tau \leqslant t}(\|\operatorname{div} \boldsymbol{\rho}_{\mathbf{u}_t}(\tau)\|^2 + \|\operatorname{div} \boldsymbol{\rho}_{\mathbf{u}_{tt}}(\tau)\|^2)
\end{aligned} \tag{43}$$

Then (42) and (43) yield

$$E(t) \leqslant E(0)\exp(-C_1 t) + \frac{1}{C_1}\sup_{\tau \leqslant t}(\|\operatorname{div} \boldsymbol{\rho}_{\mathbf{u}_t}\|^2 + \|\operatorname{div} \boldsymbol{\rho}_{\mathbf{u}_{tt}}\|^2) \tag{44}$$

Remark 3.1. From (44), the displacement and pore-pressure errors resulting from the difference between the approximate solution and the elliptic projection are bounded by the sum of two terms of different nature. The first arises from the approximation of the Stokes problem at $t = 0$ and is strongly dependent on a compatibility condition between velocity and pressure spaces: the LBB condition for mixed methods. The second contains only the error due to the elliptic projection which, due to the weak coupling of (28), (29), converges independently of the LBB condition with the rates predicted in (36), (37). As time grows, the first term decreases exponentially and, therefore, for a sufficiently large time it is dominated by the second term. Consequently, if the exact solution is sufficiently smooth such that all seminorms on the right-hand side of (36), (37) are bounded by a finite constant for all time, then the total error E converges away from the initial time with the elliptic projection rates for any conforming combination of finite element spaces. Thus, we should expect that oscillations in the pore pressure arising from an unstable approximation of the initial data tend to disappear as time goes on and, therefore, there exists a time t_0 such that even an unstable Galerkin approximation is convergent for $t \in (t_0, \infty)$.

Remark 3.2. If stable approximations, satisfying (27), are adopted for problem M_h, the first term on the right-hand side of (44) can also be estimated using the well-known analysis of mixed methods for Stokes problem and error estimates valid for the whole time domain can be derived. For example, the choice $k = l + 1 = n$ (Taylor-Hood elements) leads to[20]

$$\|\boldsymbol{\varepsilon}(\mathbf{u}(0)) - \boldsymbol{\varepsilon}(\mathbf{u}_h(0))\| + \|p(0) - p_h(0)\| \leqslant Ch^n(|\mathbf{u}(0)|_{n+1} + |p(0)|_n) \tag{45}$$

4. ERROR ESTIMATES VALID FOR THE UNBOUNDED TIME DOMAIN

For the stable choice $k = l + 1$, the authors in Reference 22 derived error estimates for problem M_{ht} which are valid for a finite time $[0, T]$. These estimates are not very accurate when $t \rightarrow \infty$, since they contain error constants that necessarily increase with time. Next we show that by exploring the decay behaviour, we can derive sharper error estimates valid for the unbounded time domain.

4.1. *Unstable Galerkin approximation*

First we focus our analysis on the unstable equal-order approximation $k = l = n$ to which the elliptic projection estimates are given by

$$\|\operatorname{div} \boldsymbol{\rho}_{\mathbf{u}_t}\| \leqslant Ch^n(|\mathbf{u}_t|_{n+1} + |p_t|_{n+1}) \tag{46}$$

$$\|\operatorname{div} \boldsymbol{\rho}_{\mathbf{u}_{tt}}\| \leqslant Ch^n(|\mathbf{u}_{tt}|_{n+1} - |p_{tt}|_{n+1}) \tag{47}$$

and using (46) and (47) in (44) we obtain

$$E(t) \leqslant E(0)\exp(-C_1 t) + Ch^s \sup_{\tau \leqslant t}((|\mathbf{u}_t|_{n+1} + |p_t|_{n+1})^2 + (|\mathbf{u}_{tt}|_{n+1} + |p_{tt}|_{n+1})^2) \tag{48}$$

Thus, for large t we can neglect the effect of the initial data in (48), and making use of the inequality

$$\|a + b\|^2 \leqslant 2(\|a\|^2 + \|b\|^2) \tag{49}$$

we obtain

$$E(t) \leqslant Ch^{2n} \sup_{\tau \leqslant t} \phi_1^2(\tau) \tag{50}$$

with

$$\phi_1^2(\tau) = |\mathbf{u}_t(\tau)|_{n+1}^2 + |p_t(\tau)|_{n+1}^2 + |\mathbf{u}_{tt}(\tau)|_{n+1}^2 + |p_{tt}(\tau)|_{n+1}^2 \tag{51}$$

From (30), (31), (41) and (49) we have

$$\begin{aligned}\|\boldsymbol{\varepsilon}(\mathbf{u}) - \boldsymbol{\varepsilon}(\mathbf{u}_h)\|^2 &+ \|\operatorname{div} \mathbf{u} - \operatorname{div} \mathbf{u}_h\|^2 + \|\nabla p - \nabla p_h\|^2 \\ &+ \|\boldsymbol{\varepsilon}(\mathbf{u}_t) - \boldsymbol{\varepsilon}(\mathbf{u}_{ht})\|^2 + \|\operatorname{div} \mathbf{u}_t - \operatorname{div} \mathbf{u}_{ht}\|^2 \\ &\leqslant 2(E + \|\boldsymbol{\varepsilon}(\boldsymbol{\rho}_{\mathbf{u}})\|^2 + \|\operatorname{div} \boldsymbol{\rho}_{\mathbf{u}}\|^2 + \|\nabla \rho_p\|^2 \\ &+ \|\boldsymbol{\varepsilon}(\boldsymbol{\rho}_{\mathbf{u}_t})\|^2 + \|\operatorname{div} \boldsymbol{\rho}_{\mathbf{u}_t}\|^2)\end{aligned} \tag{52}$$

Adding the estimate of the elliptic projection to (50) and considering (52), for sufficiently large time, we have

$$\|\boldsymbol{\varepsilon}(\mathbf{u}(t))-\boldsymbol{\varepsilon}(\mathbf{u}_h(t))\|+\|\nabla p(t)-\nabla p_h(t)\|\leqslant Ch^n\sup_{\tau\leqslant t}\phi_2(\tau) \tag{53}$$

with

$$\phi_2(\tau)=|\mathbf{u}(\tau)|_{n+1}+|p(\tau)|_{n+1}+|\mathbf{u}_t(\tau)|_{n+1}+|p_t(\tau)|_{n+1}+|\mathbf{u}_{tt}(\tau)|_{n+1}+|p_{tt}(\tau)|_{n+1} \tag{54}$$

Remark 4.1. Equation (53) shows that, for large t, the unstable equal-order Galerkin approximation converges with the same order of the elliptic projection. Denoting the time derivatives $\partial^i f/\partial t^i$ by f_{it}, if the exact solution is regular enough such that their time derivatives $\{\mathbf{u}_{it}(t), p_{it}(t)\}\in(H^{n+1}(\Omega))^2\times H^{n+1}(\Omega)$ for $0\leqslant i\leqslant 2$, then there exists a positive finite constant C such that $\sup_{\tau\leqslant t}\phi_2(\tau)\leqslant C<\infty$, and the following estimate holds away from the initial time:

$$\|\boldsymbol{\varepsilon}(\mathbf{u}(t))-\boldsymbol{\varepsilon}(\mathbf{u}_h(t))\|+\|\nabla p(t)-\nabla p_h(t)\|\leqslant Ch^n \tag{55}$$

4.2. *Stable Galerkin approximation*

For $k=l+1$ we can apply (45) to estimate the error in the initial data and a sharper error estimate for problem $\mathbf{M}_{ht}$ can be derived. However, if we pursue the previous approach, using (42), we still need to estimate $\|\boldsymbol{\varepsilon}(\mathbf{e}_{\mathbf{u}_t}(0))\|^2+\|\operatorname{div}\mathbf{e}_{\mathbf{u}_t}(0)\|^2$. To avoid this, we make use of (27) to derive a reduced decay for $\|\boldsymbol{\varepsilon}(\mathbf{e}_\mathbf{u})\|^2+\|\operatorname{div}(\mathbf{e}_\mathbf{u})\|^2+\|\nabla e_p\|^2$, valid only for stable approximations. This result can be obtained by choosing $\mathbf{v}_h=\mathbf{e}_{\mathbf{u}_t}$ in (38) and in its time derivative, $q_h=e_p+e_{pt}$ in (39), and adding them to get

$$\frac{\mathrm{d}}{\mathrm{d}t}\left(2\mu\|\boldsymbol{\varepsilon}(\mathbf{e}_\mathbf{u})\|^2+\lambda\|\operatorname{div}\mathbf{e}_\mathbf{u}\|^2+\frac{\kappa}{\eta}\|\nabla e_p\|^2\right)+4\mu\|\boldsymbol{\varepsilon}(\mathbf{e}_{\mathbf{u}_t})\|^2+2\lambda\|\operatorname{div}\mathbf{e}_{\mathbf{u}_t}\|^2$$
$$+\frac{2\kappa}{\eta}\|\nabla e_p\|^2\leqslant 2(\operatorname{div}\boldsymbol{\rho}_{\mathbf{u}_t}, e_p+e_{pt}) \tag{56}$$

To bound the right-hand side of (56), we apply the following inequality:

$$2(\operatorname{div}\boldsymbol{\rho}_{\mathbf{u}_t}, e_p+e_{pt})\leqslant\left(\frac{1}{\eta_1}+\frac{1}{\eta_2}\right)\|\operatorname{div}\boldsymbol{\rho}_{\mathbf{u}_t}\|^2+\eta_1\|e_p\|^2+\eta_2\|e_{pt}\|^2 \tag{57}$$

holding for η_1 and $\eta_2>0$. Choosing $\eta_1=\kappa/\eta\delta^2$, where δ is the constant of Poincaré inequality

$$\|e_p\|\leqslant\gamma\|\nabla e_p\| \tag{58}$$

we bound $\eta_1\|e_p\|^2$. To control $\eta_2\|e_{pt}\|^2$ we make use of the LBB condition and Cauchy–Schwarz inequality as follows:

$$\beta\|e_{pt}\|\leqslant\sup_{\mathbf{v}_h\in U_h^n}\frac{(e_{pt},\operatorname{div}\mathbf{v}_h)}{\|\nabla\mathbf{v}_h\|}=2\mu\sup_{\mathbf{v}_h\in U_h^n}\frac{(\boldsymbol{\varepsilon}(\mathbf{e}_{\mathbf{u}_t}),\boldsymbol{\varepsilon}(\mathbf{v}_h))}{\|\nabla\mathbf{v}_h\|}+\lambda\sup_{\mathbf{v}_h\in U_h^n}\frac{(\operatorname{div}\mathbf{e}_{\mathbf{u}_t},\operatorname{div}\mathbf{v}_h)}{\|\nabla\mathbf{v}_h\|}$$
$$\leqslant 2\mu\sup_{\mathbf{v}_h\in U_h^n}\frac{\|\boldsymbol{\varepsilon}(\mathbf{e}_{\mathbf{u}_t})\|\,\|\boldsymbol{\varepsilon}(\mathbf{v}_h)\|}{\|\nabla\mathbf{v}_h\|}+2\lambda\sup_{\mathbf{v}_h\in U_h^n}\frac{\|\boldsymbol{\varepsilon}(\mathbf{e}_{\mathbf{u}_t})\|\,\|\boldsymbol{\varepsilon}(\mathbf{v}_h)\|}{\|\nabla\mathbf{v}_h\|} \tag{59}$$

Hence, noting that $\|\boldsymbol{\varepsilon}(\mathbf{v}_h)\|\leqslant\|\nabla\mathbf{v}_h\|$, there exists $\alpha>0$ such that

$$\|e_{pt}\|\leqslant\alpha\|\boldsymbol{\varepsilon}(\mathbf{e}_{\mathbf{u}_t})\| \tag{60}$$

which expresses the stability of pore-pressure approximation in this case. Choosing $\eta_2=4\mu/\alpha$, the errors $\|e_p\|^2$ and $\|e_{pt}\|^2$ can be bounded by $\|\nabla e_p\|^2$ and $\|\boldsymbol{\varepsilon}(\mathbf{e}_{\mathbf{u}_t})\|^2$ in (56) and we obtain

$C_2 = (4\eta\delta^2\mu + \alpha\kappa)/4\mu\kappa$ such that

$$\frac{d}{dt}\left(2\mu \| \boldsymbol{\varepsilon}(\mathbf{e}_u) \|^2 + \lambda \| \operatorname{div} \mathbf{e}_u \|^2 + \frac{\kappa}{\eta} \| \nabla e_p \|^2\right) + \frac{\kappa}{\eta} |\nabla e_p \|^2 \leqslant C_2 \| \operatorname{div} \boldsymbol{\rho}_{u_t} \|^2 \tag{61}$$

To derive the reduced decay equation, it remains to obtain $\| \boldsymbol{\varepsilon}(\mathbf{e}_u) \|^2 + \| \operatorname{div} \mathbf{e}_u \|^2$ on the left-hand side of (61). Setting $\mathbf{v}_h = \mathbf{e}_u$ in (38) this term can be bounded by $\| \nabla e_p \|^2$ as follows:

$$\begin{aligned} 2\mu \| \boldsymbol{\varepsilon}(\mathbf{e}_u) \|^2 + \lambda \| \operatorname{div} \mathbf{e}_u \|^2 = (e_p, \operatorname{div} \mathbf{e}_u) &\leqslant \frac{1}{2\eta_3} \| e_p \|^2 + \frac{\eta_3}{2} \| \operatorname{div} \mathbf{e}_u \|^2 \\ &\leqslant \frac{1}{2\eta_3} \delta^2 \| \nabla e_p \|^2 + \frac{\eta_3}{2} \| \operatorname{div} \mathbf{e}_u \|^2 \end{aligned} \tag{62}$$

Choosing $\eta_3 = \lambda$, we conclude that there exists $C_3 = (\lambda/2\delta^2)\max(4\mu, \lambda)$ such that

$$\| \nabla e_p \|^2 = \frac{\| \nabla e_p \|^2}{2} + \frac{\| \nabla e_p \|^2}{2} \geqslant \frac{\| \nabla e_p \|^2}{2} + \frac{C_3}{2} (\| \boldsymbol{\varepsilon}(\mathbf{e}_u) \|^2 + \| \operatorname{div} \mathbf{e}_u \|^2) \tag{63}$$

Therefore, from (61), (63) and defining C_1 and C_2 appropriately, a reduced decay expression can be obtained in the form

$$\frac{d}{dt}(\| \boldsymbol{\varepsilon}(\mathbf{e}_u) \|^2 + \| \operatorname{div} \mathbf{e}_u \|^2 + \| \nabla e_p \|^2) + C_1(\| \boldsymbol{\varepsilon}(\mathbf{e}_u) \|^2 + \| \operatorname{div} \mathbf{e}_u \|^2 + |\nabla e_p \|^2 \leqslant C_2 \| \operatorname{div} \boldsymbol{\rho}_{u_t} \|^2 \tag{64}$$

from which, using (34), one obtains

$$\| \boldsymbol{\varepsilon}(\mathbf{e}_u(t) \|^2 + \| \nabla e_p(t) \|^2 \leqslant C\{\exp(-C_1 t)(\| \boldsymbol{\varepsilon}(\mathbf{e}_u(0)) \|^2 + \| \nabla e_p(0) \|^2) + \sup_{\tau \leqslant t} \| \operatorname{div} \boldsymbol{\rho}_{u_t}(\tau) \|^2\} \tag{65}$$

To estimate the initial data error, we consider that

$$\begin{aligned} \| \boldsymbol{\varepsilon}(\mathbf{e}_u(0)) \|^2 + \| \nabla e_p(0) \|^2 \leqslant 2(\| \boldsymbol{\varepsilon}(\mathbf{u}(0)) - \boldsymbol{\varepsilon}(\mathbf{u}_h(0)) \|^2 + \| \boldsymbol{\varepsilon}(\boldsymbol{\rho}_u(0)) \|^2 \\ + \| \nabla p(0) - \nabla p_h(0) \|^2 + \nabla \rho_p(0) \|^2) \end{aligned} \tag{66}$$

and for the left-hand side of (65) we have

$$\begin{aligned} \| \boldsymbol{\varepsilon}(\mathbf{u}(t)) - \boldsymbol{\varepsilon}(\mathbf{u}_h(t)) \|^2 + \| \nabla p(t) - \nabla p_h(t) \|^2 \leqslant 2(\| \boldsymbol{\varepsilon}(\mathbf{e}_u(t)) \|^2 \\ + \| \nabla e_p(t) \|^2 + \| \boldsymbol{\varepsilon}(\boldsymbol{\rho}_u(t)) \|^2 + \nabla \rho_p(t) \|^2) \end{aligned} \tag{67}$$

Considering (45) and adopting the same previous procedure, we derive

$$\| \boldsymbol{\varepsilon}(\mathbf{u}(t)) - \boldsymbol{\varepsilon}(\mathbf{u}_h(t)) \| + \| \nabla p(t) - \nabla p_h(t) \| \leqslant Ch^{n-1} \sup_{\tau \in (0, \infty)} \phi_3(\tau) \tag{68}$$

with

$$\phi_3(\tau) = |\mathbf{u}(\tau)|_{n+1} + |\mathbf{u}_t(\tau)|_{n+1} + |p(\tau)|_n + |p_t(\tau)|_n \tag{69}$$

Estimate (68) extends, to the unbounded time domain, results obtained in Reference 22 for a finite time interval $(0, T]$. For $\| \boldsymbol{\varepsilon}(\mathbf{u} - \mathbf{u}_h) \|$, (68) is suboptimal with gap one compared to the corresponding elliptic projection (equation (33)). However, we can derive a sharper decay result for $\|\varepsilon(\mathbf{e}_\mathbf{u})\|$ by choosing $\mathbf{v}_h = \mathbf{e}_{\mathbf{u}_t}$ in (38), $q_h = e_p$ in (39) to obtain C_1 and $C_2 > 0$ such that

$$\frac{\mathrm{d}}{\mathrm{d}t}(\|\varepsilon(\mathbf{e}_\mathbf{u})\|^2 + \|\operatorname{div}\mathbf{e}_\mathbf{u}\|^2) + C_1(\|\varepsilon(\mathbf{e}_\mathbf{u})\|^2 + \|\operatorname{div}\mathbf{e}_\mathbf{u}\|^2) \leqslant C_2\|\operatorname{div}\boldsymbol{\rho}_{\mathbf{u}_t}\|^2 \tag{70}$$

yielding

$$\|\varepsilon(\mathbf{e}_\mathbf{u}(t))\| \leqslant C\{\exp(-C_1 t)\|\varepsilon(\mathbf{e}_\mathbf{u}(0))\| + \sup_{\tau\leqslant t}\|\operatorname{div}\boldsymbol{\rho}_{\mathbf{u}_t}(\tau)\|\} \tag{71}$$

leading to the estimate

$$\|\varepsilon(\mathbf{u}(t)) - \varepsilon(\mathbf{u}_h(t))\| \leqslant Ch^n \sup_{\tau\leqslant t}\phi_3(\tau) \tag{72}$$

which is optimal, in the sense of having the same order of convergence of the elliptic projection.

Remark 4.2. From (68), (69) and (72) we note that contrary to (53), no regularity is required for the second time derivative of the exact solution. To satisfy the required regularity $\sup_{\tau\leqslant t}\phi_3(\tau)\leqslant C$ for uniform convergence of Taylor-Hood approximation we only need $\{\mathbf{u}_{it}(t), p_{it}(t)\}\in(H^{n+1}(\Omega))^2\times H^n(\Omega)$ for $i = 0, 1$.

5. DECAY FUNCTIONS FOR THE FULLY DISCRETE APPROXIMATION

Let Δt be the time step and $\{\mathbf{u}_h^m, p_h^m\}$ the approximation of $\{\mathbf{u}(t), p(t)\}$ at $t_m = m\Delta t$. The stable backward Euler operator ∂_t approximates the time derivative by the quotient $\partial_t\mathbf{u}^m = (\mathbf{u}^m - \mathbf{u}^{m-1})\Delta t^{-1}$. Thus, the fully discrete backward Euler-Galerkin approximation of problem M_t is given by

Problem M_h^m. For each time step $m\Delta t$, $m\geqslant 1$, find $\{\mathbf{u}_h^m, p_h^m\}\in U_h^k\times V_h^l$ such that

$$2\mu(\varepsilon(\mathbf{u}_h^m), \varepsilon(\mathbf{v}_h)) + \lambda(\operatorname{div}\mathbf{u}_h^m, \operatorname{div}\mathbf{v}_h) - (p_h^m, \operatorname{div}\mathbf{v}_h) = f(\mathbf{v}_h) \quad \forall\mathbf{v}_h\in U_h^k \tag{73}$$

$$(\operatorname{div}\mathbf{u}_h^m, q_h) + \frac{\kappa\Delta t}{\eta}(\nabla p_h^m, \nabla q_h) = (\operatorname{div}\mathbf{u}_h^{m-1}, q_h) + \Delta t g(q_h) \quad \forall q_h\in V_h^l \tag{74}$$

with $\mathbf{u}_h^0$ and p_h^0 satisfying

M_{h0}.

$$2\mu(\varepsilon(\mathbf{u}_h^0), \varepsilon(\mathbf{v}_h)) - (p_h^0, \operatorname{div}\mathbf{v}_h) = f(\mathbf{v}_h) \quad \forall\mathbf{v}_h\in U_h^k \tag{75}$$

$$(\operatorname{div}\mathbf{u}_h^0, q_h) = 0 \quad \forall q_h\in V_h^l \tag{76}$$

Similarly to the semidiscrete case, we set

$$\|\mathbf{u}(t_m) - \mathbf{u}_h^m\| \leqslant \|\boldsymbol{\rho}_\mathbf{u}^m\| + \|\mathbf{e}_\mathbf{u}^m\| \tag{77}$$

$$\|p(t_m) - p_h^m\| \leqslant \|\rho_p^m\| + \|e_p^m\| \tag{78}$$

with $\boldsymbol{\rho}_\mathbf{u}^m$ and ρ_p^m representing the difference between the exact solution and the elliptic projection, and $\mathbf{e}_\mathbf{u}^m$ and e_p^m the difference between the elliptic projection and the approximate solution at $t = t_m$. For the elliptic projection we have

$$\|\varepsilon(\boldsymbol{\rho}_\mathbf{u}^m)\| \leqslant Ch^s(|\mathbf{u}(t_m)|_{k+1} + |p(t_m)|_{l+1}) \tag{79}$$

$$\|\nabla\rho_p^m\| \leqslant Ch^l|p(t_m)|_{l+1} \tag{80}$$

In this case the variational error equation is given by

$$2\mu(\varepsilon(\mathbf{e}_\mathbf{u}^m), \varepsilon(\mathbf{v}_h)) + \lambda(\operatorname{div}\mathbf{e}_\mathbf{u}^m, \operatorname{div}\mathbf{v}_h) - (e_p^m, \operatorname{div}\mathbf{v}_h) = 0 \quad \forall\mathbf{v}_h\in U_h^k \tag{81}$$

$$(\operatorname{div}(\partial_t \mathbf{e}_u^m), q_h) + \frac{\kappa}{\eta}(\nabla e_p^m, \nabla q_h) = (\operatorname{div} \boldsymbol{\omega}^m, q_h) \quad \forall q_h \in V_h^l \tag{82}$$

where

$$\boldsymbol{\omega}^m = \mathbf{u}_t(t_m) - \partial_t \overline{\mathbf{u}_h^m} \tag{83}$$

Similarly, as in the semidiscrete case, let

$$E^m = \|\boldsymbol{\varepsilon}(\mathbf{e}_u^m)\|^2 + \|\operatorname{div} \mathbf{e}_u^m\|^2 + \|\nabla e_p^m\|^2 + \|\boldsymbol{\varepsilon}(\partial_t \mathbf{e}_u^m)\|^2 + \|\operatorname{div} \partial_t \mathbf{e}_u^m\|^2 \tag{84}$$

A fully discrete decay result for E^m can be derived setting $\mathbf{v}_h = \partial_t \mathbf{e}_u^m$ in (81), $q_h = e_p^m + \partial_t e_p^m$ in (82) and $\mathbf{v}_h = \partial_t \mathbf{e}_u^m + \partial_t^2 \mathbf{e}_u^m$, $q_h = \partial_t e_p^m$ in their respective backward Euler-differenced forms, to obtain

$$\begin{aligned}
&2\mu((\boldsymbol{\varepsilon}(\mathbf{e}_u^m), \boldsymbol{\varepsilon}(\partial_t \mathbf{e}_u^m)) + \|\boldsymbol{\varepsilon}(\partial_t \mathbf{e}_u^m)\|^2 + (\boldsymbol{\varepsilon}(\partial_t \mathbf{e}_u^m), \boldsymbol{\varepsilon}(\partial_t^2 \mathbf{e}_u^m))) + \lambda((\operatorname{div} \mathbf{e}_u^m, \operatorname{div} \partial_t \mathbf{e}_u^m) \\
&\quad + \|\operatorname{div} \partial_t \mathbf{e}_u^m\|^2 + (\operatorname{div} \partial_t \mathbf{e}_u^m, \operatorname{div} \partial_t^2 \mathbf{e}_u^m)) + \frac{\kappa}{\eta}(\|\nabla e_p^m\|^2 + (\nabla e_p^m, \nabla \partial_t e_p^m) + \|\nabla \partial_t e_p^m\|^2) \\
&= (\operatorname{div} \boldsymbol{\omega}^m, e_p^m + \partial_t e_p^m) + (\operatorname{div} \partial_t \boldsymbol{\omega}^m, \partial_t e_p^m)
\end{aligned} \tag{85}$$

Noting that

$$\begin{aligned}
(A^m, \partial_t A^m) &= \Delta t^{-1}(\|A^m\|^2 - (A^m, A^{m-1})) \\
&\geqslant \Delta t^{-1}(\|A^m\|^2 - \tfrac{1}{2}\|A^m\|^2 - \tfrac{1}{2}\|A^{m-1}\|^2) = \tfrac{1}{2}\partial_t \|A^m\|^2
\end{aligned} \tag{86}$$

and using (57) and (86) in (85), we have

$$\begin{aligned}
&\partial_t(\mu(\|\boldsymbol{\varepsilon}(\mathbf{e}_u^m)\|^2 + \|\boldsymbol{\varepsilon}(\partial_t \mathbf{e}_u^m)\|^2) + \frac{\lambda}{2}(\|\operatorname{div} \mathbf{e}_u^m\|^2 + \|\operatorname{div} \partial_t \mathbf{e}_u^m\|^2) + \frac{\kappa}{2\eta}\|\nabla e_p^m\|^2) \\
&\quad + 2\mu\|\boldsymbol{\varepsilon}(\partial_t \mathbf{e}_u^m)\|^2 + \lambda\|\operatorname{div} \partial_t \mathbf{e}_u^m\|^2 + \frac{\kappa}{\eta}(\|\nabla e_p^m\|^2 + \|\nabla \partial_t e_p^m\|^2) \\
&\leqslant \frac{1}{2\eta_1}\|\operatorname{div} \boldsymbol{\omega}^m\|^2 + \eta_1(\|e_p^m\|^2 + \|\partial_t e_p^m\|^2) + \frac{1}{2\eta_2}\|\operatorname{div} \partial_t \boldsymbol{\omega}^m\|^2 + \frac{\eta_2}{2}\|\partial_t e_p^m\|^2
\end{aligned} \tag{87}$$

Applying Poincaré inequality (58) to bound the right-hand side of (87) and choosing η_1 and η_2 appropriately, we obtain

$$\begin{aligned}
&\partial_t\left(\mu(\|\boldsymbol{\varepsilon}(\mathbf{e}_u^m)\|^2 + \|\boldsymbol{\varepsilon}(\partial_t \mathbf{e}_u^m)\|^2) + \frac{\lambda}{2}(\|\operatorname{div} \mathbf{e}_u^m\|^2 + \|\operatorname{div} \partial_t \mathbf{e}_u^m\|^2) + \frac{\kappa}{2\eta}\|\nabla e_p^m\|^2\right) \\
&\quad + 2\mu\|\boldsymbol{\varepsilon}(\partial_t \mathbf{e}_u^m)\|^2 + \lambda\|\operatorname{div} \partial_t \mathbf{e}_u^m\|^2 + \frac{\kappa}{\eta}(\|\nabla e_p^m\|^2 + \|\nabla \partial_t e_p^m\|^2) \\
&\leqslant C_4(\|\operatorname{div} \boldsymbol{\omega}^m\|^2 + \|\operatorname{div} \partial_t \boldsymbol{\omega}^m\|^2)
\end{aligned} \tag{88}$$

with $C_4 > 0$. Similar to (63), we set $\mathbf{v}_h = \mathbf{e}_u^m$ in (81) to obtain $C_3 > 0$ such that

$$\|\nabla e_p^m\|^2 \geqslant \frac{\|\nabla e_p^m\|^2}{2} + \frac{C_3}{2}(\|\boldsymbol{\varepsilon}(\mathbf{e}_u^m)\|^2 + \|\operatorname{div} \mathbf{e}_u^m\|^2) \tag{89}$$

Thus, from (88), (89) and appropriate definitions of C_1 and C_2, we have

$$\partial_t E^m + C_1 E^m \leqslant C_2(\|\operatorname{div} \boldsymbol{\omega}^m\|^2 + \|\operatorname{div} \partial_t \boldsymbol{\omega}^m\|^2) \tag{90}$$

The above inequality is similar to (40), with time derivative replaced by Euler operator, and can be written as

$$(1 + C_1\Delta t)E^m \leqslant E^{m-1} + C_2\Delta t(\|\operatorname{div}\boldsymbol{\omega}^m\|^2 + \|\operatorname{div}\partial_t\boldsymbol{\omega}^m\|^2) \tag{91}$$

which expresses the unconditional stability of the adopted time discretization, as demonstrated in Reference 13 using the spectral decomposition approach. Considering that

$$\partial_t(E^m(1 + C_1\Delta t)^m) = (1 + C_1\Delta t)^{m-1}(\partial_t E^m + C_1 E^m) \tag{92}$$

we note that $(1 + C_1\Delta t)^{m-1}$ is the "integration factor' of (90), which can be written as

$$\partial_t(E^m(1 + C_1\Delta t)^m) \leqslant C_2(1 + C_1\Delta t)^{m-1}(\|\operatorname{div}\boldsymbol{\omega}^m\|^2 + \|\operatorname{div}\partial_t\boldsymbol{\omega}^m\|^2) \tag{93}$$

or, equivalently

$$(1 + C_1\Delta t)^m E^m - (1 + C_1\Delta t)^{m-1}E^{m-1} \leqslant C_2\Delta t(1 + C_1\Delta t)^{m-1}(\|\operatorname{div}\boldsymbol{\omega}^m\|^2 + \|\operatorname{div}\partial_t\boldsymbol{\omega}^m\|^2) \tag{94}$$

Adding (94) for all time steps we get

$$(1 + C_1\Delta t)^m E^m \leqslant E^0 + C_2\Delta t\sum_{j=1}^{m}(1 + C_1\Delta t)^{j-1}(\|\operatorname{div}\boldsymbol{\omega}^j\|^2 + \|\operatorname{div}\partial_t\boldsymbol{\omega}^j\|^2) \tag{95}$$

yielding

$$E^m \leqslant (1 + C_1\Delta t)^{-m}E^0 + C_2\Delta t\sum_{j=1}^{m}(1 + C_1\Delta t)^{j-1-m}(\|\operatorname{div}\boldsymbol{\omega}^j\|^2 + \|\operatorname{div}\partial_t\boldsymbol{\omega}^j\|^2) \tag{96}$$

Equation (96) expresses the decay of the influence of E^0 over E^m in time for problem M_h^m. Noting that $\Delta t = t_m/m$, for each m the associated decay function $f_m(t_m)$ is given by

$$f_m(t_m) = \left(\frac{m}{m + C_1 t_m}\right)^m \tag{97}$$

Taking the limit $m \to \infty$, the exponential decay function f_∞ of the semidiscrete case is recovered as follows:

$$\begin{aligned}\ln f_\infty(t_m) &= \lim_{m\to\infty}\ln f_m(t_m) = \lim_{m\to\infty} m\ln\left(\frac{m}{m + C_1 t_m}\right)\\ &= \lim_{m\to\infty}\frac{\ln(m/(m + C_1 t_m))}{1/m} = -\lim_{m\to\infty}\frac{C_1 t_m m}{m + C_1 t_m} = -C_1 t_m\end{aligned} \tag{98}$$

implying

$$f_\infty(t_m) = \exp(-C_1 t_m) \tag{99}$$

In Figure 1 we present an illustration of the behaviour of $f_m(t_m)$ for different values of m.

Up to the error in the initial data, exploring the decay in (96), we can derive error estimates for problem M_h^m valid over the unbounded time domain. Neglecting the effect of the error in the initial data, for sufficiently large time, we have

$$E^m \leqslant C_2\sum_{j=1}^{m}\Delta t(1 + C_1\Delta t)^{j-1-m}(\|\operatorname{div}\boldsymbol{\omega}^j\|^2 + \|\operatorname{div}(\partial_t\boldsymbol{\omega}^j)\|^2). \tag{100}$$

To estimate $\boldsymbol{\omega}^m$, we set

$$\begin{aligned}\boldsymbol{\omega}^j &= \mathbf{u}_t(t_j) - \partial_t\bar{\mathbf{u}}_h(t_j) = \mathbf{u}_t(t_j) - \partial_t\mathbf{u}(t_j) + \partial_t\mathbf{u}(t_j) - \partial_t\bar{\mathbf{u}}_h(t_j)\\ &= \mathbf{u}_t(t_j) - \partial_t\mathbf{u}(t_j) + \partial_t\,\boldsymbol{\rho}_{\mathbf{u}}^j = \boldsymbol{\omega}_2^j + \boldsymbol{\omega}_1^j\end{aligned} \tag{101}$$

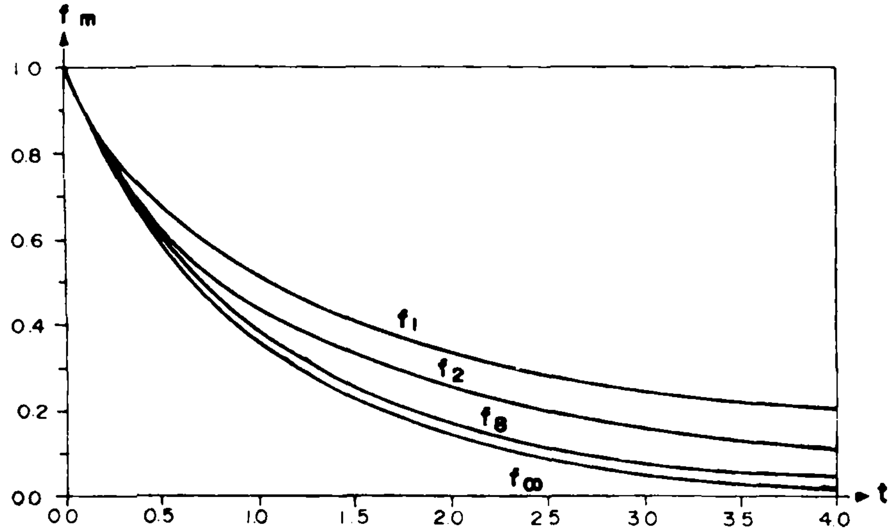

Figure 1. Behaviour of the family of decay functions f_m for $C_1 = 1$

where the terms $\boldsymbol{\omega}_1^j$, $\boldsymbol{\omega}_2^j$ result from the elliptic projection and time-derivative approximations. Considering the estimate of $\|\operatorname{div}\boldsymbol{\rho}_{\mathbf{u}_t}\|$ we get

$$\begin{aligned}\|\operatorname{div}\boldsymbol{\omega}_1^j\| &= \Delta t^{-1}\left\|\int_{t_{j-1}}^{t_j}\operatorname{div}\boldsymbol{\rho}_{\mathbf{u}_t}\,d\tau\right\| \leqslant \Delta t^{-1}\int_{t_{j-1}}^{t_j}\|\operatorname{div}\boldsymbol{\rho}_{\mathbf{u}_t}\|\,d\tau\\ &\leqslant C\Delta t^{-1}h^s\int_{t_{j-1}}^{t_j}|\mathbf{u}_t|_{k+1}+|p_t|_{l+1}\,d\tau \leqslant Ch^s\sup_{\tau\in(t_{j-1},t_j)}(|\mathbf{u}_t(\tau)|_{k+1}+|p_t(\tau)|_{l+1})\end{aligned} \tag{102}$$

For $\|\operatorname{div}\omega_2^j\|$, applying Cauchy–Schwarz inequality, we have

$$\begin{aligned}\|\operatorname{div}\boldsymbol{\omega}_2^j\| &= \Delta t^{-1}\left\|\int_{t_{j-1}}^{t_j}(\tau-t_{j-1})\operatorname{div}\mathbf{u}_{tt}\,d\tau\right\| \leqslant \Delta t^{-1}\int_{t_{j-1}}^{t_j}\|(\tau-t_{j-1})\operatorname{div}\mathbf{u}_{tt}\|\,d\tau\\ &\leqslant \int_{t_{j-1}}^{t_j}\|\operatorname{div}\mathbf{u}_{tt}\|\,d\tau \leqslant \left(\int_{t_{j-1}}^{t_j}\|\operatorname{div}\mathbf{u}_{tt}\|^2\,d\tau\right)^{1/2}\left(\int_{t_{j-1}}^{t_j}1\,d\tau\right)^{1/2}\\ &= \Delta t^{1/2}\left(\int_{t_{j-1}}^{t_j}\|\operatorname{div}\mathbf{u}_{tt}\|^2\,d\tau\right)^{1/2} \leqslant \Delta t\sup_{\tau\in(t_{j-1},t_j)}\|\operatorname{div}\mathbf{u}_{tt}(\tau)\|\end{aligned} \tag{103}$$

A similar estimate for $\|\operatorname{div}(\partial_t\omega^j)\|$ can be obtained as follows:

$$\|\operatorname{div}(\partial_t\boldsymbol{\omega}^j)\| = \Delta t^{-1}\left\|\int_{t_{j-1}}^{t_j}\operatorname{div}\boldsymbol{\omega}_t^j\,d\tau\right\| \leqslant \Delta t^{-1}\int_{t_{j-1}}^{t_j}\|\operatorname{div}\boldsymbol{\omega}_t^j\|\,d\tau \leqslant \sup_{\tau\in(t_{j-1},t_j)}\|\operatorname{div}\boldsymbol{\omega}_t^j(\tau)\| \tag{104}$$

which when combined with the time derivative of estimates (102) and (103), leads to

$$\|\operatorname{div}(\partial_t\boldsymbol{\omega}^j)\| \leqslant C(h^s+\Delta t)\sup_{\tau\in(t_{j-1},t_j)}(|\mathbf{u}_{tt}(\tau)|_{k+1}+|p_{tt}(\tau)|_{l+1}+\|\operatorname{div}\mathbf{u}_{ttt}(\tau)\|) \tag{105}$$

Therefore, adding (102), (103) and (105) for all steps and using (49) in (100) we derive

$$E^m \leqslant C(h^{2s} + (\Delta t)^2) \sup_{\tau \in (0, \infty)} \phi_4^2(\tau) \sum_{j=1}^{m} \Delta t(1 + C_1 \Delta t)^{j-1-m} \tag{106}$$

where

$$\phi_4^2(\tau) = |\mathbf{u}_t(\tau)|_{k+1}^2 + |p_t(\tau)|_{l+1}^2 + |(\mathbf{u}_{tt}(\tau)|_{k+1}^2 + |p_{tt}(\tau)|_{l+1}^2 + \|\operatorname{div} \mathbf{u}_{tt}(\tau)\|^2 + \|\operatorname{div} \mathbf{u}_{ttt}(\tau)\|^2 \tag{107}$$

Thus, to obtain estimates with $O(h^s + \Delta t)$, it remains to prove that for all $m = 1, 2, \ldots$ the series in (106) is bounded by a constant, independently of Δt. In fact we have

$$\sum_{j=1}^{m} \Delta t(1 + C_1 \Delta t)^{j-1-m} \leqslant \sum_{i=1}^{m} \Delta t(1 + C_1 \Delta t)^{-i} \leqslant \sum_{i=1}^{\infty} \Delta t(1 + C_1 \Delta t)^{-i} \tag{108}$$

$$\leqslant \sum_{i=0}^{\infty} \Delta t(1 + C_1 \Delta t)^{-i} - 1) = \Delta t \left(\frac{1}{1 - 1/(1 + C_1 \Delta t)} - 1 \right) = \frac{1}{C_1} \tag{109}$$

Consequently, for sufficiently large time, we obtain

$$\|\boldsymbol{\varepsilon}(\mathbf{e}_{\mathbf{u}}^m)\| + \|\nabla e_p^m\| \leqslant C(h^s + \Delta t) \sup_{\tau \in (0, \infty)} \phi_4(\tau) \tag{110}$$

As before, estimates for $\|\boldsymbol{\varepsilon}(\mathbf{u}(t_m) - \mathbf{u}_h^m)\|$ and $\|\nabla(p(t) - p_h^m)\|$ can easily be obtained by adding estimates of $\|\boldsymbol{\varepsilon}(\boldsymbol{\rho}_{\mathbf{u}}^m)\|$ and $\|\nabla \rho_p^m\|$ to (110). For the unstable equal-order method $k = l = n$,

$$\|\boldsymbol{\varepsilon}(\mathbf{u}(t_m)) - \boldsymbol{\varepsilon}(\mathbf{u}_h^m)\| \leqslant C(h^n + \Delta t) \sup_{\tau \in (0, \infty)} \phi_5(\tau) \tag{111}$$

$$\|\nabla p(t_m) - \nabla p_h^m\| \leqslant C(h^n + \Delta t) \sup_{\tau \in (0, \infty)} \phi_5(\tau) \tag{112}$$

with

$$\begin{aligned}\phi_5(\tau) = {} & |(\mathbf{u}(\tau)|_{n+1} + |p(\tau)|_{n+1} + |(\mathbf{u}_t(\tau)|_{n+1} + |p_t(\tau)|_{n+1} + |(\mathbf{u}_{tt}(\tau)|_{n+1} \\ & + |p_{tt}(\tau)|_{n+1} + \|\operatorname{div} \mathbf{u}_{tt}(\tau)\| + \|\operatorname{div} \mathbf{u}_{ttt}(\tau)\|\end{aligned} \tag{113}$$

Remark 5.1. As in the semidiscrete case, assuming the necessary regularity for the exact solution (at least $\{\mathbf{u}_{it}(t), p_{it}(t)\} \in (H^{n+1}(\Omega))^2 \times H^{n+1}(\Omega)$, for $0 \leqslant i \leqslant 2$ and $\|\operatorname{div} \mathbf{u}_{ttt}\| \in L^2(\Omega)$), there exists $C > 0$ such that $\sup_{\tau \leqslant t} \phi_5(\tau) \leqslant C < \infty$ for $0 < t < \infty$ and consequently, for a sufficiently large time, we have the estimate

$$\|\boldsymbol{\varepsilon}(\mathbf{u}(t_m)) - \boldsymbol{\varepsilon}(\mathbf{u}_h^m)\| + \|\nabla p(t_m) - \nabla p_h^m\| \leqslant C(h^n + \Delta t) \tag{114}$$

which is the fully discrete analogue of (55). It says that, for large t, the completely discrete equal order Euler Galerkin scheme converges, independently of the LBB condition, with the same order of the elliptic projection in h, and first order in Δt. We also observe that, for large Δt, the spatial convergence, is polluted by time discretization, causing destruction of the h-rates, and *viceversa*, i.e. the pollution caused by spatial discretization on Δt-rates, for large h.

Applying the same methodology of the semidiscrete case, we can derive error estimates for stable methods ($k = l + 1 = n$), extending for $t \in (0, \infty)$ the results presented in References 22. In this case we have the following fully discrete estimates:

$$\|\boldsymbol{\varepsilon}(\mathbf{u}(t_m) - \boldsymbol{\varepsilon}(\mathbf{u}_h^m)\| \leqslant C(h^n + \Delta t) \sup_{\tau\in(0,\infty)} \phi_6(\tau) \tag{115}$$

$$\|\nabla p(t_m) - \nabla p_h^m\| \leqslant C(h^l + \Delta t) \sup_{\tau\in(0,\infty)} \phi_6(\tau) \tag{116}$$

with

$$\phi_6(\tau) = |\mathbf{u}(\tau)|_{n+1} + |p(\tau)|_n + |\mathbf{u}_t(\tau)|_{n+1} + |p_t(\tau)|_n + \|\operatorname{div} \mathbf{u}_{tt}(\tau)\| \tag{117}$$

6. POST-PROCESSING TECHNIQUE

We now consider a post-processing technique for the pore pressure with the same order of interpolation of displacement approximation that can be adopted even close to $t = 0$. This technique consists in, after obtaining the solution of problem M_h^m with the stable approximation $k = l + 1$, reconsidering (74) to obtain a new approximation for pore pressure P_h^m by solving the following problem.

Problem G_h^m. For given $\mathbf{u}_h^m$, solution of problem M_h^m with $k = l + 1$, find $P_h^m \in V_h^k$ such that

$$\frac{\kappa}{\eta}(\nabla P_h^m, \nabla q_h) + (\partial_t \operatorname{div} \mathbf{u}_h^m, q_h) = g(q_h) \quad \forall q_h \in V_h^k \tag{118}$$

For the semidiscrete Galerkin approximation of (118), in Reference 22 we derived error estimates for a finite time interval $[0, T]$, demonstrating an improvement in the pore-pressure accuracy compared to the direct approximation obtained with Taylor–Hood elements. Exploring the decay for $\|\operatorname{div} \mathbf{u}_t(t_m) - \operatorname{div} \partial_t \mathbf{u}_h^m\|$, up to the initial data term $\|\operatorname{div} \mathbf{u}_t(0) - \operatorname{div} \partial_t \mathbf{u}_h^0\|$, we can derive error estimates for $\|\nabla p(t) - \nabla P_h^m\|$ also valid for the unbounded time domain. Considering (118) and (119) with $q = q_h$, we show that

$$\|\nabla p(t_m) - \nabla P_h^m\| \leqslant C\{\|\nabla p(t_m) - \nabla q_h\| + \|\operatorname{div} \mathbf{u}_t(t_m) - \operatorname{div} \partial_t \mathbf{u}_h^m\|\} \quad \forall q_h \in V_h^k \tag{119}$$

Similarly to (115), adopting $k = l + 1 = n$, for $\|\boldsymbol{\varepsilon}(\mathbf{u}_t(t_m)) - \boldsymbol{\varepsilon}(\partial_t \mathbf{u}_h^m)\|$, for sufficiently large time we have

$$\|\operatorname{div} \mathbf{u}_t(t_m) - \operatorname{div} \partial_t \mathbf{u}_h^m\| \leqslant \sqrt{2}\|\boldsymbol{\varepsilon}(\mathbf{u}_t(t_m)) - \boldsymbol{\varepsilon}(\partial_t \mathbf{u}_h^m)\| \leqslant C(h^n + \Delta t) \sup_{\tau\in(0,\infty)} \phi_{6t}(\tau) \tag{120}$$

Therefore, from (119), (120) and according to the interpolation theory, we derive

$$\|\nabla p(t_m) - \nabla P_h^m\| \leqslant C(h^n + \Delta t) \sup_{\tau\in(0,\infty)} \phi_7(\tau) \tag{121}$$

with

$$\phi_7 = \phi_{6t} + |p|_{n+1} \tag{122}$$

Remark 6.1. For $t \in (t_0, \infty)$, the post-processed pore pressure P_h^m converges with order n while the Taylor–Hood approximation p_h^m converges with order $n - 1$. So, an improvement of accuracy is obtained compared to stable methods.

Remark. 6.2. In the numerical examples, presented next, we illustrate that the post-processing technique can also be applied to obtain a stable equal-order biquadratic approximation for the pore pressure in the early stages of the consolidation process.

Remark 6.3. When solving problem G_h^m, the given displacement $\mathbf{u}_h^m$ should be obtained using a stable Taylor Hood approximation of M_h^m. Otherwise, misbehaviour, such as locking phenomena, usually frequent in unstable velocity approximation in the Stokes problem, will destroy the convergence of the post-processing for short time.

7. NUMERICAL RESULTS

Numerical experiments were performed to validate the present analysis. First, we solve the classical column problem, using its well-known analytical solution[26] to verify the predicted rates of convergence. Second, a uniform strip-load consolidation of clay layer underlain by a fixed impervious base is considered to illustrate the performance of the methods in a two-dimensional example.

7.1. One-dimensional consolidation

This problem consists of a porous column bounded by rigid and impermeable walls, except on its top, where it is loaded by a pressure p_0, and free to drain. The boundary and initial conditions are

$$\sigma = -p_0, \quad p = 0 \quad \text{on } x = 0 \tag{123}$$

$$u = 0, \quad \frac{\partial p}{\partial x} = 0 \quad \text{on } x = H \tag{124}$$

$$\frac{\partial u}{\partial x} = 0 \quad \text{in } (0, H), \quad t = 0 \tag{125}$$

and, in non-dimensional form, the analytical solution is given by

$$u^* = 1 - x^* - \sum_{n=0}^{\infty} \frac{2}{M^2} \cos(Mx^*) e^{-M^2 t^*} \tag{126}$$

$$p^* = \sum_{n=0}^{\infty} \frac{2}{M} \sin(Mx^*) e^{-M^2 t^*} \tag{127}$$

where

$$x^* = x/H, \quad t^* = (\lambda + 2\mu)kt/\eta H^2, \quad M = \pi(2n+1)/2 \tag{128}$$

$$u^* = u(\lambda + 2\mu)/p_0 H, \quad p^* = p/p_0 \tag{129}$$

For each time, the post-processed pore pressure is obtained using a three-node quadratic interpolation after an evolution adopting the lowest stable Taylor–Hood three-node quadratic element for displacement and two-node linear (continuous) for the pore pressure. To verify the rates of convergence we considered uniform meshes of 2, 4, 8, 16, 32 elements and a small $\Delta t^* = 5 \times 10^{-5}$ to avoid pollution of the h-convergence by the time-domain discretization. Figures 2 and 3 compare the accuracy and convergence rates between the post-processed pore pressure and the stable Taylor–Hood approximation. Due to the existence of a boundary layer close to $x = 0$ (Figure 2) in the beginning of the consolidation process which leads to non-smooth solutions for small t, both methods are inaccurate close to the boundary layer. This fact does not occur for large time, when the exact solution becomes smooth and a great improvement of convergence of the post-processing compared to the classical stable method is verified (Figures 3(a) and 3(b)). The gradient of the post-processed pore pressure converges with order h^2, while the Taylor–Hood approximation converges with order h. As $t \to 0$, the stability properties of both methods are preserved but, due to the lack of regularity of the exact solution, both methods do not exhibit optimal rates of convergence Figures 3(c) and 3(d).

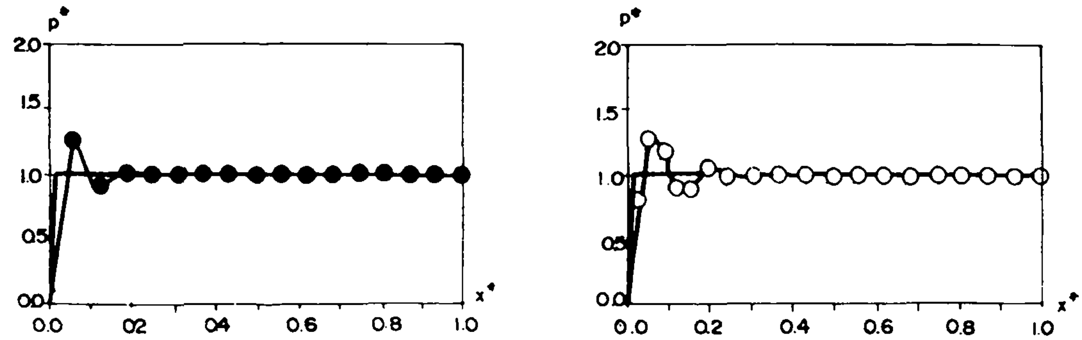

Figure 2. Accuracy of pore-pressure approximations: ' - ' analytical solution; '—●—' Taylor–Hood approximation; '—○—' post-processing approach ($t^* = 10^{-6}$)

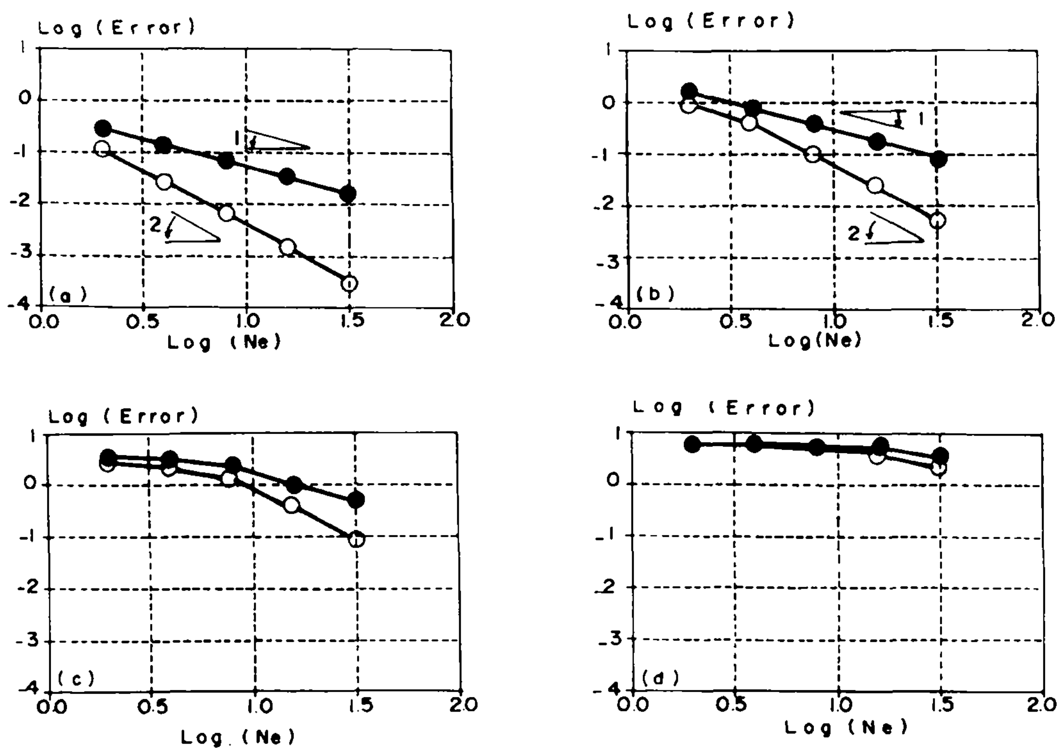

Figure 3. h-convergence of $\|\nabla p - \nabla p_h\|$: ' ● ' Taylor–Hood approximation; '—○—' post-processing approach. (a) $t^* = 10^{-1}$; (b) $t^* = 10^{-2}$, (c) $t^* = 10^{-3}$, (d) $t^* = 10^{-4}$

Figure 4 compares the pore-pressure accuracy obtained with quadratic equal-order approximation and the post-processed one, for two different uniform meshes and non-smooth solutions ($t^* = 10^{-6}$). Contrary to the post-processing, for course grids (Figures 4(a) and 4(b)) the unstable equal-order method exhibits oscillations propagating through the whole domain which reduce with refinement (Figures 4(c) and 4(d)). Figure 5 shows the accuracy and h-convergence of the

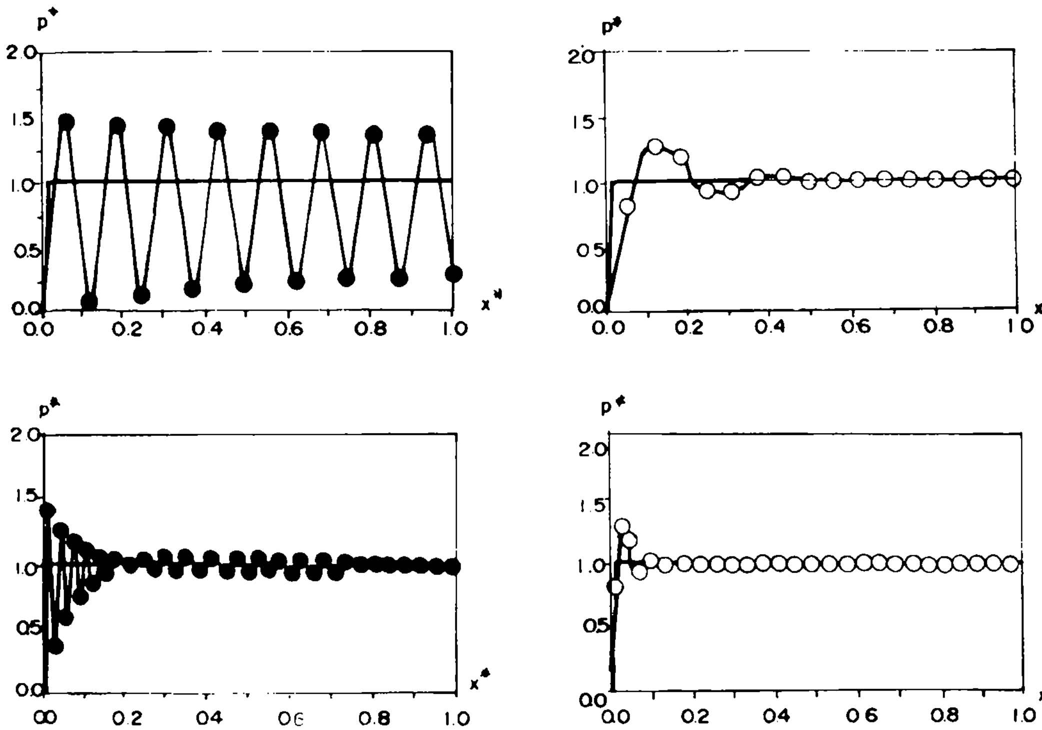

Figure 4. Accuracy of pore-pressure approximations: '——' analytical solution; '—●—' unstable equal-order quadratic approximation; '○' post-processing approach; (a) 8 elements (b) 32 elements ($t^* = 10^{-6}$)

pore pressure for both methods at large time, when the exact solution has the necessary regularity and the effect of the initial data error is negligible. Due to the decay, both methods exhibit good accuracy and optimal rates of convergence of order h^2 for the gradient.

7.2. Two-dimensional true consolidation

The performance of the previous methods is also illustrated in a classical true consolidation situation consisting of a uniform strip-load consolidation of a clay layer (half width $a = 20$ m, height $H = 5a = 100$ m) underlain by a fixed impervious base (Figure 6). Young's modulus and Poisson's ratio of the clay are, respectively, $E = 0{\cdot}3 \times 10^5$ N/m^2 and $\nu = 0{\cdot}2$ and the percolation coefficient was chosen $\kappa/\eta = 10^{-7}$ m^4/Ns.

First, we evaluate the whole time of consolidation t_c employing uniform mesh of 15×15 biquadratic elements for displacements and bilinear for pore pressure. Adopting $\Delta t \cong 7$ h in the time-domain discretization, we obtain $t_c \cong 2$ yr, according to the criterion

$$\min_{0<t<\infty} \max_{\Omega} \left(\frac{p(t - t_c)}{\max_\Omega p(t = 0)} \right) \leqslant 0{\cdot}02 \tag{130}$$

Figure 7 presents the evolution of the pore-pressure field as a function of the time, obtained with a unstable equal-order approximation of 30×30 bilinear elements for both displacements and pore pressure and $\Delta t = 1$ min.

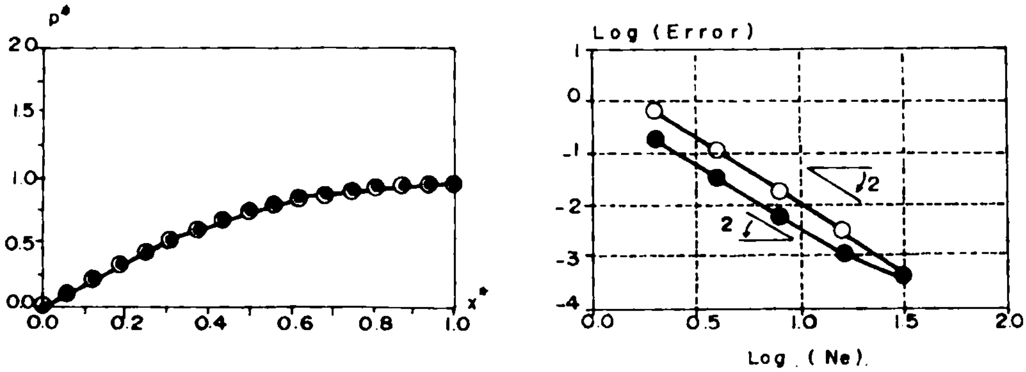

Figure 5. Accuracy and h-convergence of $\|\nabla p - \nabla p_h\|$: '—— —' analytical solution; '—●— ' unstable equal-order quadratic approximation; '- -○- ' post-processing approach ($t^* = 10^{-1}$)

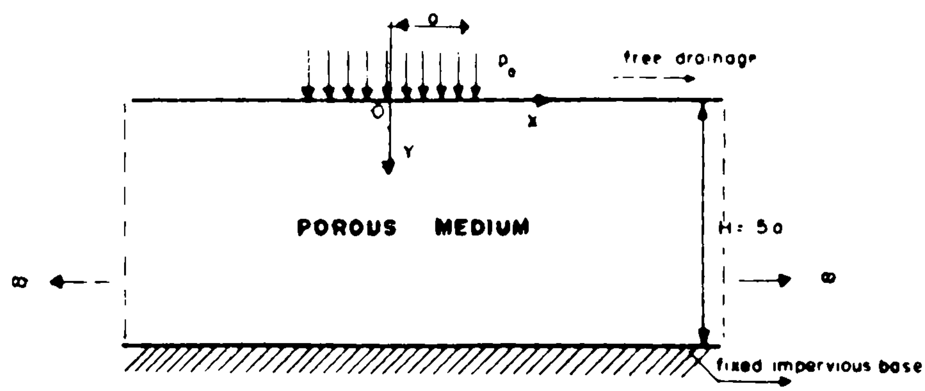

Figure 6. Classical bidimensional strip-load consolidation problem

No oscillations are observed for $t \geqslant 500$ min. Figure 8 compares the pore-pressure oscillations at the centreline of the strip load for two different time steps. Note that the reduction of the oscillations, related to the change of the decay function, occurs as a consequence of the decrease of the time step.

Figure 9 illustrates the application of the post-processing technique in the stabilization of the initial pore pressure. Also for $\Delta t = 1$ min, the post-processed pore pressure is obtained employing a uniform mesh of 15×15 biquadratic elements after a stable evolution adopting Taylor–Hood biquadratic displacement and bilinear pore-pressure element. Significant improvement of stability and accuracy compared to the equal-order approximation is achieved in the early stages of the consolidation process.

Figure 10 shows the evolution in time of the difference between unstable and post-processed pore pressures for two values of the number of time steps using a biquadratic interpolation. According to the previous analysis, the decay is verified and also an acceleration of the decay process occurs as a consequence of the refinement of the time domain.

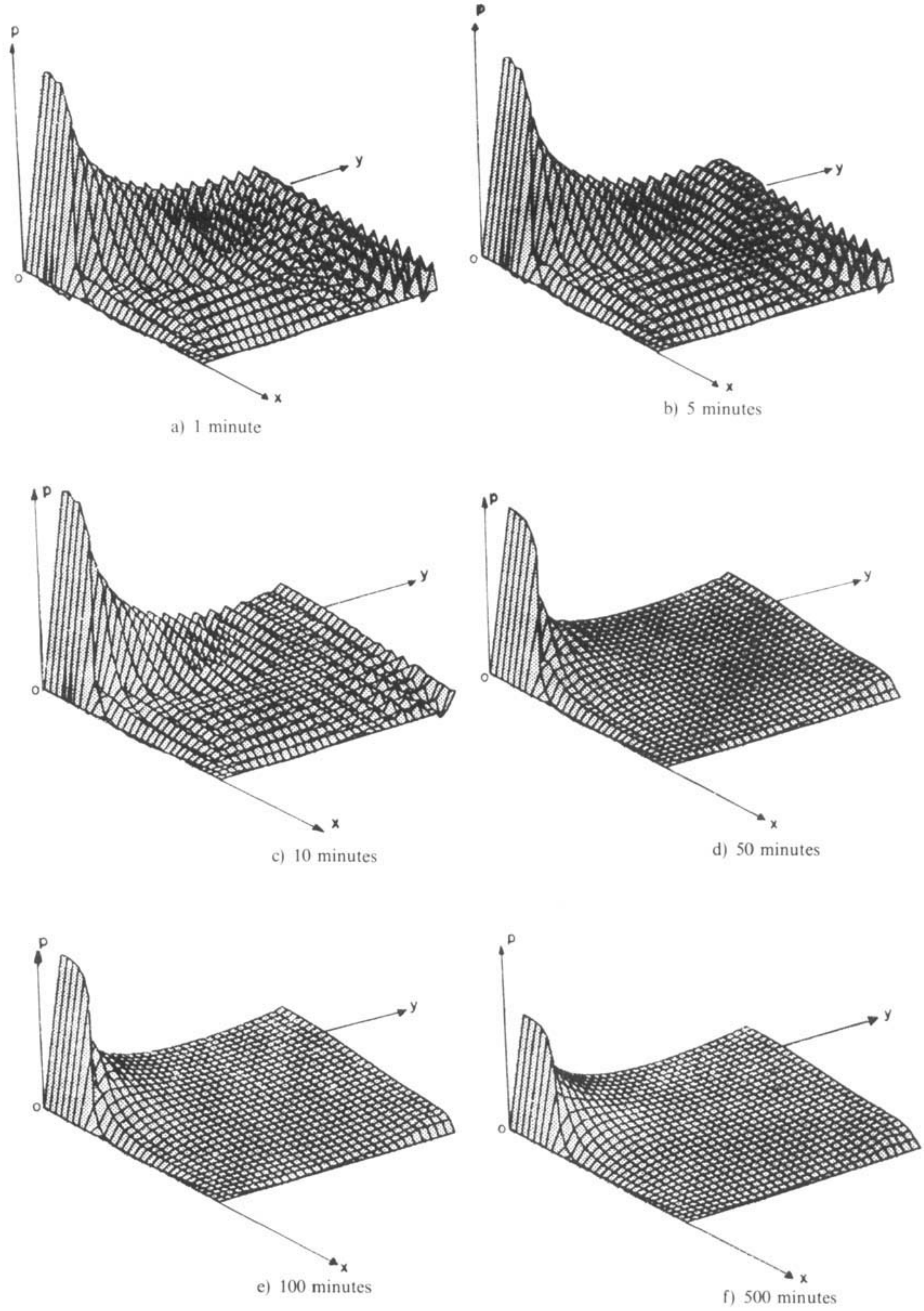

Figure 7. Evolution of pore-pressure oscillations in a true consolidation situation

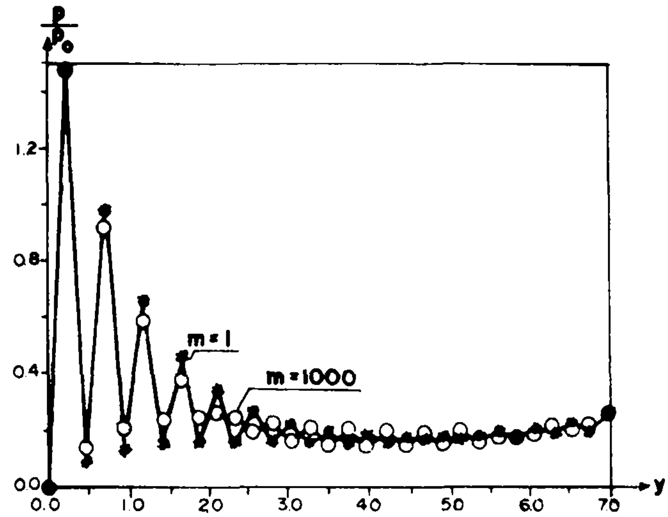

Figure 8. Pore-pressure oscillations at $x = 0$ (t = 100 min.)

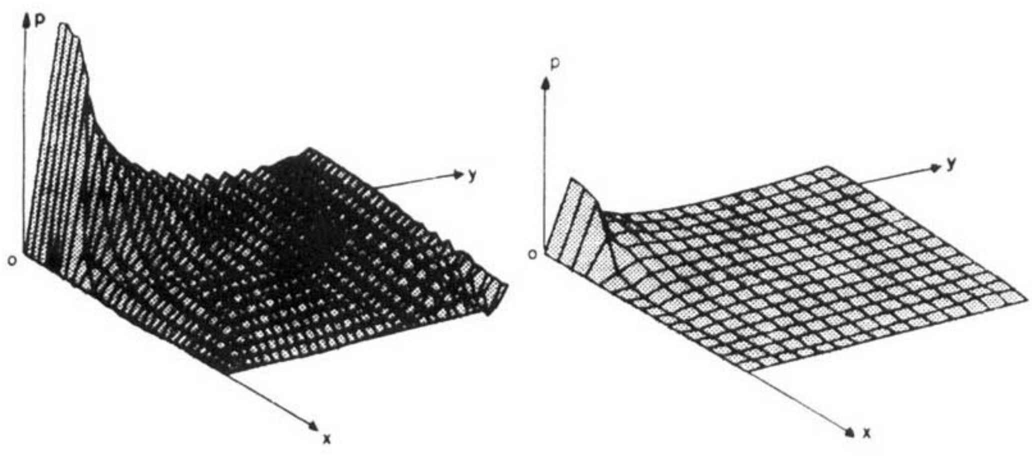

a) Unstable

b) Post-Processed

Figure 9. Comparison between unstable and post-processed pore pressures (t = 10 min.)

8. CONCLUSIONS

Stability and convergence analysis of finite element approximations of Biot's consolidation problem are presented and error estimates, valid for the unbounded time domain, are derived for both semidiscrete and fully discrete Galerkin formulations.

For sufficiently large time, due to the exponential decay, the influence of the initial data becomes negligible and optimal rates of convergence, with the same order of the elliptic projection, are proved for any combination of the finite element spaces for displacement and pore-pressure fields, independently of the LBB condition.

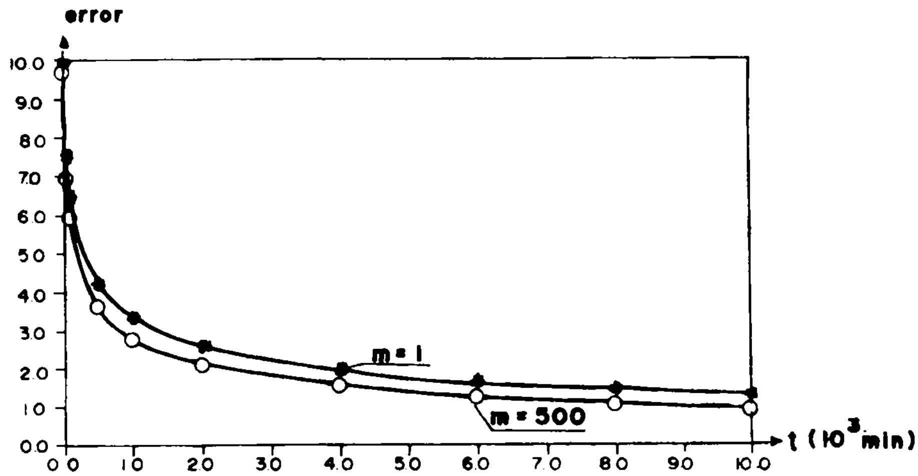

Figure 10. Evolution of $\|\nabla P_h^m - \nabla p_h^m\|$

To improve the accuracy of the pore-pressure approximation, a post-processing technique is adopted, reconsidering the moment equation for the pore fluid, using the same order of displacement interpolation.

For stable methods, considering that the initial data error is given by the numerical analysis of Stokes problem, error estimates over $0 \leqslant t \leqslant \infty$ are derived, leading to lower accuracy for the pore pressure compared to the displacement approximation.

For the fully discrete backward Euler–Galerkin approximation, a family of decay functions, parametrized by the number of the time steps, is derived and the exponential decay function is recovered as the number of time steps tends to infinity.

Numerical experiments in one- and two-dimensional consolidation problems were performed to verify the predicted rates of convergence and to illustrate the improved accuracy of the post-processed pore pressure.

REFERENCES

1. M. Biot, 'General theory of three dimensional consolidation', *J. Appl. Phys.*, **12**, 155–164 (1941)
2. M. Biot, 'Theory of elasticity and consolidation for a porous anisotropic solid', *J. Appl. Phys.*, **26**, 182–185 (1955).
3. M. Biot, 'General solutions of the equations of elasticity and consolidation for a porous material', *J. Appl. Mech.*, **78**, 91 96 (1956).
4. M. Biot and D. G. Willis, 'The elastic coefficient of the theory of consolidation', *J. Appl. Mech.*, **79**, 594–601 (1957).
5. J. R. Booker, 'A numerical method for the solution of Biot's consolidation theory', *Quart. J. Mech. Appl. Math.*, **XXVI**, 457 470 (1973).
6. R. I. Borja, 'Finite element formulation for transient pore pressure dissipation: a variational approach', *Int. J. Solids Struct.*, **22**, 1201 1211 (1986).
7. C. T. Hwang, N. R. Morgenstern and D. W. Murray, 'On solutions of plane strain consolidation problems by finite element methods', *Can. Geotech. J.*, **8**, 109–118 (1971).
8. C. T. Hwang, N. R. Morgenstern and D. S. Murray, 'Application of the Finite Element Method to Consolidation Problems', *Proc. Symp. Applications of the Finite Method in Geotech. Eng.*, Vicksberg, Mississippi, 1972, pp. 735–756.
9. R. S. Sandhu and E. L. Wilson, 'Finite element analysis of seepage in elastic media', *J. Eng. Mech. Div. ASCE*, **95**, 641 652 (1969).
10. Y. Yokoo, K. Yamagata and H. Nagaoka, 'Variational principles for consolidation', *Soils Found.*, **11**(4), 25 35 (1971).
11. Y. Yokoo, K. Yamagata and H. Nagaoka, 'Finite element method applied to Biot's consolidation theory', *Soils Found.*, **11**(1), 29 -46 (1971).

12. J. R. Booker and J. C. Small, 'An investigation of the stability of numerical solutions of Biot's equations of consolidation', *Int. J. Solids Struct.*, **11**, 907–917 (1975).
13. R. W. Lewis and B. A. Schrefler, *The Finite Element Method in the Deformation and Consolidation of Porous Media*, Wiley, Chichester, 1987.
14. P. A. Vermeer and A. Verruut, 'An accuracy condition for consolidation by finite elements', *Int. j. numer anal. methods geomech.*, **5**, 1–14 (1981).
15. W. K. Nukulchal and V. W. Suaris, 'An efficient finite element scheme for elastic porous media', *Int. J. Solids Struct.*, **18**(1), 37–49 (1982).
16. M. B. Reed, 'An investigation of numerical errors in the analysis of consolidation by finite elements', *Int. j. numer anal. methods geomech.*, **8**, 243–257 (1984).
17. R. S. Sandhu, H. Liu and K. J. Singh, 'Numerical performance of some finite element schemes for analysis of seepage in porous elastic media', *Int. j. numer anal. methods geomech.*, **1**, 177–194 (1977).
18. F. Brezzi, 'On the existence, uniqueness and approximation of saddle-point problems arising from Lagrange multipliers', *RAIRO, Anal. Numér.*, **8**(R-2), 129 151 (1974).
19. M. Fortin, 'Old and new finite elements for incompressible flows', *Int. j. numer. methods fluids*, **1**, 347 364 (1983).
20. V. Girault and P. A. Raviart, *Finite Element Methods for Navier–Stokes Equations*, Springer, New York, 1986.
21. J. T. Oden and O. P. Jacquotte, 'Stability of some finite element methods for Stokesian flows', *Comput. Methods Appl. Mech. Eng.*, **43**, 231–247 (1984).
22. M. A. Murad and A. F. D. Loula, 'Improved accuracy in finite element analysis of Biot's consolidation problem', *Comput. Methods Appl. Mech. Eng.*, **95**, 359–382 (1992).
23. V. Thomée, 'Galerkin finite element methods for parabolic problems', *Lecture Notes in Mathematics 1054*, Springer, Berlin, 1984.
24. C. Taylor and P. Hood, 'A numerical solution of the Navier Stokes equations using the finite element technique', *Comput. Fluids*, **1**, 73–100 (1973).
25. P. G. Ciarlet, *The Finite Element Method for Elliptic Problems*, North-Holland, Amsterdam, 1978.
26. K. Terzaghi, *Theoretical Soil Mechanics*, Wiley, New York, 1942.
27. O. Axelson and V. A. Baker, *Finite Element Solution of Boundary Value Problems: Theory and Computation*, Academic Press, New York, 1984.
28. E. Duvaut and J. L. Lions, *Inequalities in Mechanics and Physics*, Springer, New York, 1976.
29. M. A. Murad, 'Modelling and numerical analysis of saturated flows in rigid and linear elastic porous media', *D.Sc. Thesis*, Pontificia Universidade Católica do Rio de Janeiro, 1990.